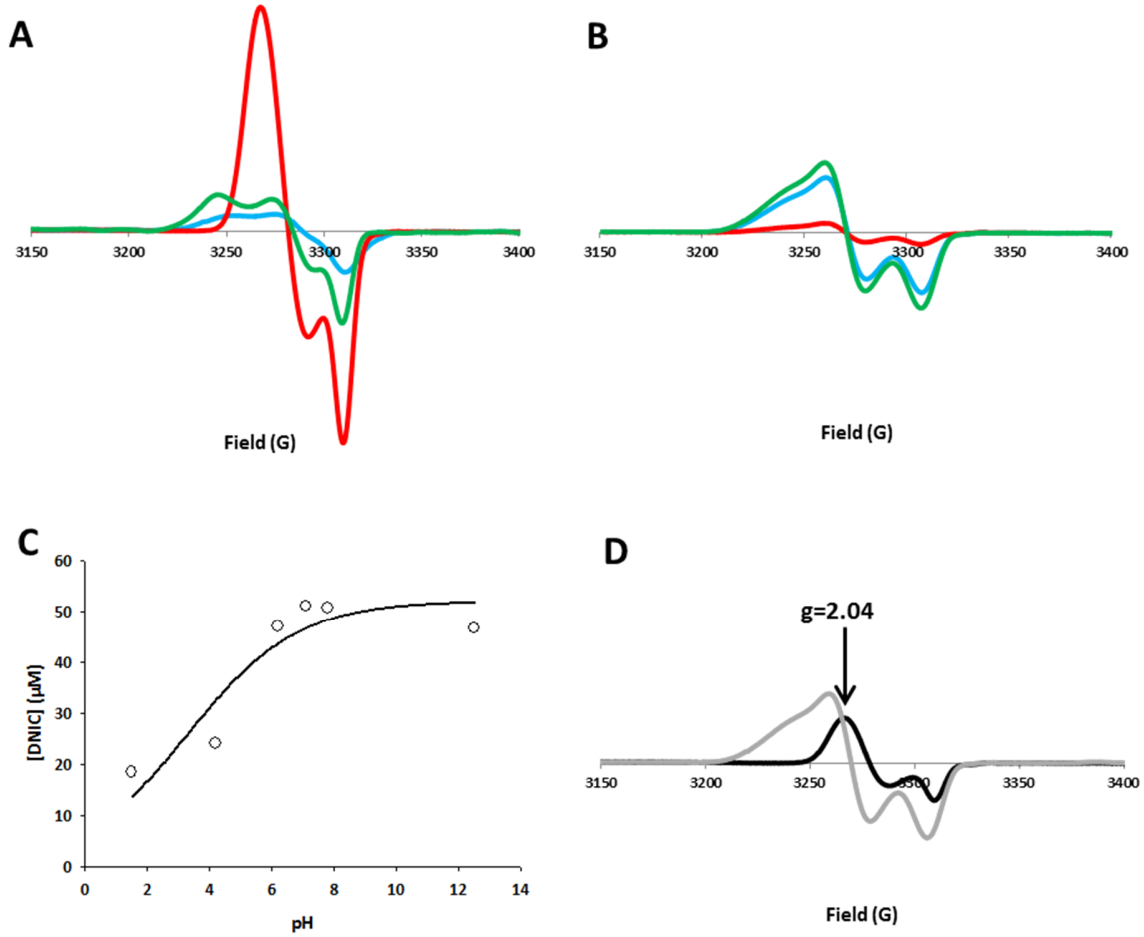

Supplementary Figure 1. Influence of anion ligands and pH on EPR spectra of DNIC. (**A**): Spectra of DNIC from $FeSO_4$, Proli/NO in 10 mM PBS (green), 15 mM Hepes (blue), and with cysteine in 15 mM Hepes (Fe:Cys=1:20) (red); pH 7.4 in each case. (**B**): Same as in (A) with 10 % of 2 N HCl addition to the DNIC samples. (**C**): Intensity of DNIC (Fe:Cys=1:20, in 15 mM Hepes) spectra as a function of pH. (**D**): Spectra of DNIC from $FeSO_4$, Proli/NO and cysteine (Fe:Cys=1:20) in 10 mM PBS at pH 7.4 (black), and with 10 % of 2 N HCl (grey).

The DNIC formed from Hepes or PBS in the absence of cysteine exhibited an altered shape of the EPR spectrum, but did not lose paramagnetic intensity. When Cys-DNIC

was prepared in PBS, acidification resulted in change of shape, but not intensity (D). The shape change was consistent with a transformation from axial to rhombic symmetry [8] indicative of thiolate ligand displacement by phosphate at low pH. The results suggest that the binding of thiolate is much stronger than that of the sulfonate ligand in Hepes, while phosphate is competitive with thiolate at low pH. The practical conclusion from these observations is that the effect of acidification on DNIC is buffer–dependent, and the paramagnetic nature of these compounds is preserved in phosphate, but decreased in Hepes. For these reasons, all further experiments were performed in Hepes buffer.

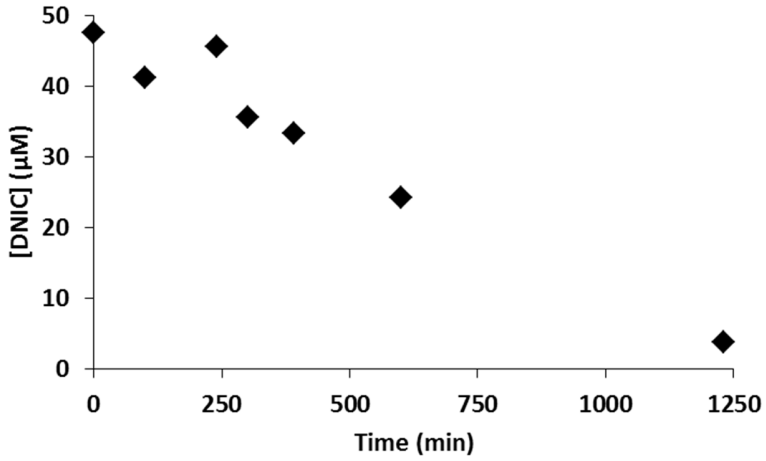

Supplementary Figure 2. Decay of mono-DNIC followed by EPR. DNIC was synthesized from 100 µM of $FeSO_4$, and 100 µm of Proli/NO with GSH (Fe:GSH=1:20) in 15 mM Hepes pH=7.4, and the kinetics of DNIC was followed with EPR.

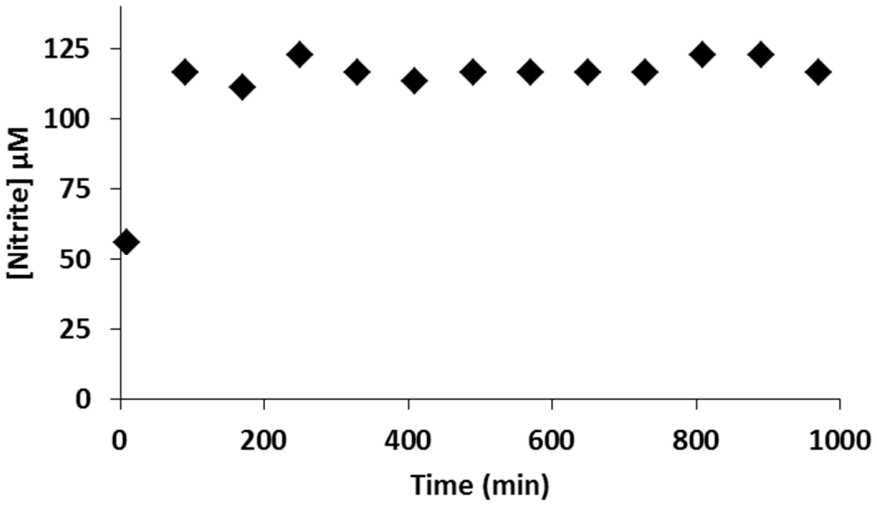

Supplementary Figure 3. **Decomposition of DNIC made with excess thiol in the presence of $HgCl_2$ at neutral pH.** DNIC was synthesized from 100µM of $FeSO_4$, and 100 µm of Proli/NO with GSH in 15 mM Hepes pH 7.4, Fe:thiol=1:20. Nitrite was detected with reverse phase HPLC/UV-Vis detector.

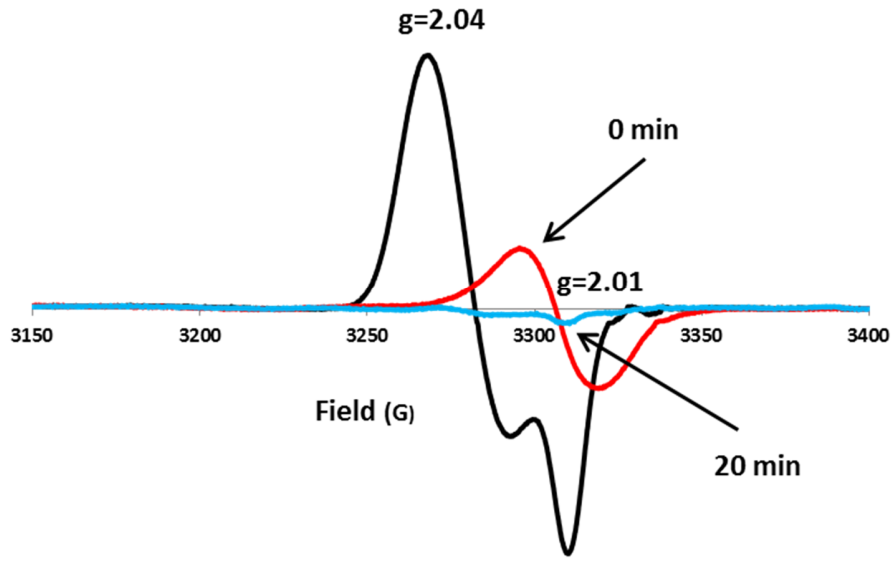

Supplementary Figure 4. **Effect of mercury chloride on mono-DNIC.** DNIC (Fe:GSH=1:20) in 15 mM Hepes pH 7.4 was monitored with EPR before and after addition of $HgCl_2$ solution. Spectra were recorded from freshly synthesized DNIC (black), immediately after $HgCl_2$ (red) addition, and 20 min later (blue). Time points are indicated with arrows.

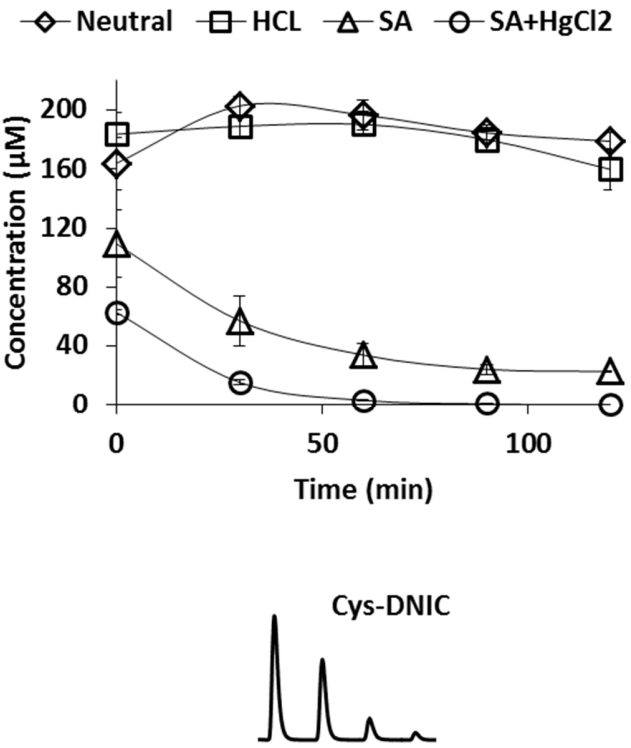

Supplementary Figure 5. Detection of DNIC with triiodide-dependent ozone-based chemiluminescence. DNIC was synthesized from 100 µM of $FeSO_4$, and 100 µm of Proli/NO with cysteine (Fe:Cys=1:2) in 15 mM Hepes pH=7.4. Upper panel: Time dependence of detected NO as GSNO equivalent, Diamonds: no additive, squares: addition of 10% 2N HCl, triangles: addition of 10% sulfanilamide, circles: addition of 10% $HgCl_2$ solution and 10% sulfanilamide. Lower panel: Chemiluminescence traces. Data are reported as mean±standard error, N=3.

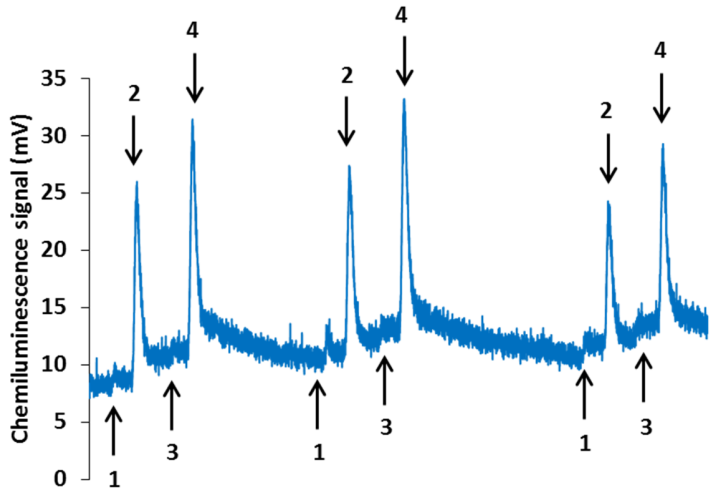

Supplementary Figure 6: Nitric oxide formation during mercury-assisted decay of DNIC. Chemiluminescence traces after injection of (1) DNIC (1:2) and (2) DNIC (1:2) after addition of $HgCl_2$, and (3) DNIC (1:20) and (4) DNIC (1:20) after addition of $HgCl_2$ The purge vessel contains only 15 mM Hepes pH 7.4.

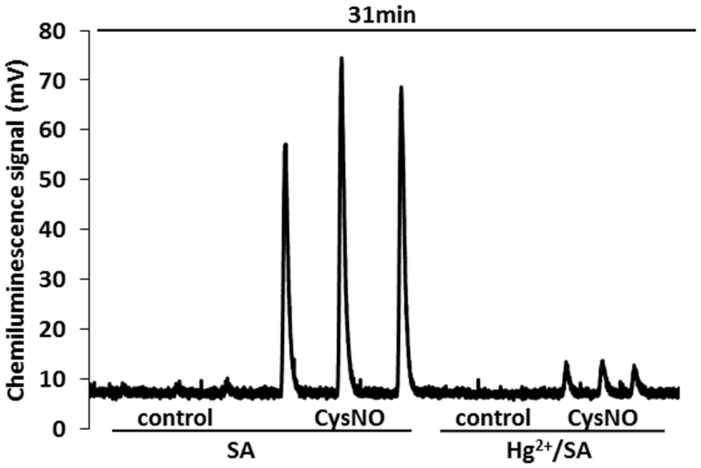

Supplementary Figure 7: Chemiluminescence traces of MCF7 cells (control and treated with 100 µm CysNO for 2 h). Quantification of peaks is shown in Figure 4F.

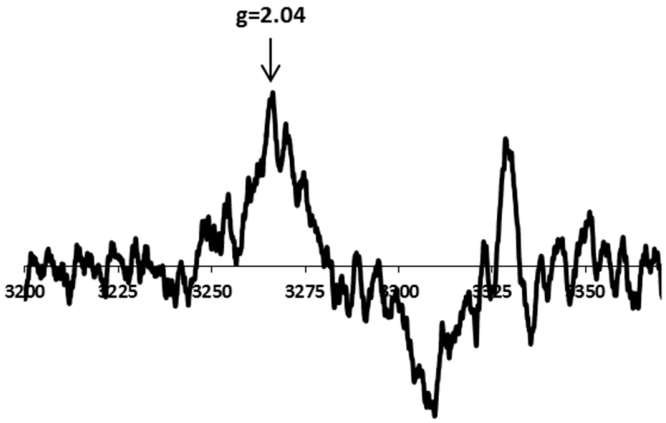

Supplementary Figure 8: EPR spectrum detected in RAW 264.7 macrophages. Cells were treated with LPS for 13 h, and then after scraping into 15 mM Hepes were put into EPR tube and snap-froze in liquid nitrogen.